In vivo photocontrol of orexin receptors with a nanomolar light-regulated analogue of orexin-B

Davia Prischich[1,2,⊢], Rosalba Sortino[1,2], Alexandre Gomila-Juaneda[1,2,#], Carlo Matera[1,2,‡], Salvador Guardiola[3,†], Diane Nepomuceno[4], Monica Varese[3,††], Pascal Bonaventure[4], Luis de Lecea[5,6], Ernest Giralt[3,7], Pau Gorostiza[1,2,8,*]

1. Institute for Bioengineering of Catalonia (IBEC), Barcelona Institute of Science and Technology, Barcelona, Spain
2. Centro de Investigación Biomédica en Red – Bioingeniería, Biomateriales y Nanomedicina (CIBER-BBN), Barcelona, Spain
3. Institute for Research in Biomedicine (IRB Barcelona), Barcelona Institute of Science and Technology, Barcelona, Spain
4. Janssen Research & Development L.L.C., San Diego, California, United States
5. Department of Psychiatry and Behavioral Sciences, School of Medicine, Stanford University, Stanford, California, United States
6. Wu Tsai Neurosciences Institute, Stanford University, Stanford, California, USA
7. Department of Inorganic and Organic Chemistry, University of Barcelona (UB), Barcelona, Spain
8. Catalan Institution for Research and Advanced Studies (ICREA), Barcelona, Spain

⊢ Department of Chemistry, Molecular Sciences Research Hub, Imperial College London, London, United Kingdom
Present address: Department of Organic Chemistry, University of Barcelona, Barcelona, Spain
‡ Present address: Department of Pharmaceutical Sciences, University of Milan, Milan, Italy
† Present address: ONA Therapeutics, Barcelona, Spain
†† Present address: OMAKASE Consulting, Barcelona, Spain

(*) E-mail: pau@icrea.cat (P.G.)

Abstract

Orexinergic neurons are critically involved in regulating arousal, wakefulness, and appetite. Their dysfunction has been associated with sleeping disorders, and non-peptide drugs are currently being developed to treat insomnia and narcolepsy. Yet, no light-regulated agents are available to reversibly control their activity. To meet this need, a photoswitchable peptide analogue of the endogenous neuroexcitatory peptide orexin-B was designed, synthesized, and tested *in vitro* and *in vivo*. This compound (photorexin) is the first photo-reversible ligand reported for orexin receptors. It allows dynamic control of activity *in vitro* (including full agonism, nanomolar activity, and subtype selectivity to human OX_2 receptors) and *in vivo* in zebrafish larvae by direct application in water. Photorexin induces dose- and light-dependent changes in locomotion and a reduction in the successive induction reflex that is associated with sleep behavior. Molecular dynamics calculations indicate that *trans* and *cis* photorexins adopt similar bent conformations and that the only discriminant between their structures and activities is the positioning of the N-terminus at the extracellular region of the orexin receptor. Thus, our approach could be extended to a broad and important family of neuropeptides that share a "message-address" mechanism when binding to their cognate receptors.

Introduction

Optical methods, and optogenetics in particular, have revolutionized neuroscience by aiding our understanding of brain circuits through light-mediated monitoring and/or manipulation of neuronal activity.[1,2] Despite broad applications in terms of targeted pathways, optogenetics has several limitations.[3] While photocontrol over the exogenous light-sensitive opsins is robust, viral expression in tissues can display poor homogeneity and specificity. Moreover, the kinetics of light-gated channels differ from those of endogenous receptors and their overexpression might lead to unintended neuroplastic phenomena. Finally, irreversible optogenetic manipulations are subject to safety and regulatory requirements that hamper or slow down their therapeutic potential.[4] In recent years, photopharmacology has emerged as a complementary approach to

control with light the function of endogenous proteins as well as lipids and ribonucleic acids.[5,6] The method relies on incorporating a photoswitchable moiety into the structure of a bioactive compound and regulating the local concentration of (in)active drug through reversible illumination.[7,8] In principle, the metabolism, pharmacokinetics, and safety of the compounds can be characterized as for conventional drugs and biologicals, in contrast to genetic manipulation methods.[8] Despite the versatility and attractiveness of the approach, many endogenous targets are still "orphan" of synthetic photoswitches.[9] In particular neuropeptides, and consequently their corresponding G protein-coupled receptors (GPCRs), have received limited attention compared to small molecule synthetic analogues of neuronal protein ligands.

Among these, a family of neuroexcitatory peptides known as orexins (or hypocretins)[10,11] is critically involved in regulating sleep and wakefulness,[12] energy homeostasis, and reward.[10] Orexin signaling is mediated by two closely related GPCRs – orexin receptor types 1 and 2 (OX_1 and OX_2), which are strongly conserved among mammals.[10,13] While orexin cell bodies are concentrated in the hypothalamic area,[10,11] orexin receptors are widely expressed in the central nervous system (CNS).[14,15] Their endogenous ligands are two peptides, named orexin-A (OX-A) and -B (OX-B), which bind to the cognate receptors with different selectivity profiles. OX-A displays high affinity towards both receptors, whereas OX-B is selective for OX_2.[10] In both cases agonist activity is transduced into a robust rise in intracellular calcium concentration.[16,17] Drug-like antagonists are currently being developed as safe insomnia treatments,[18,19] whereas disfunctions of the orexinergic system have been associated with narcolepsy.[20–22] Nonetheless, the discovery of non-peptide agonists has been challenging despite some progress,[23–25] thus providing limited structure-activity relationships[23,26] and few scaffolds to build light-regulated azologs.[27,28] Besides, these compounds might find limited applications as orexin receptors are widely expressed in the CNS. Consequently, their activity would suffer from poor spatiotemporal selectivity and might cause adverse effects. Here we present a light-regulated analogue of the orexin-B peptide, which can be reversibly toggled between two isomeric states characterized by different potencies at the orexin receptors.

Results and discussion

As revealed by 2D NMR spectroscopy, both orexin isoforms present relatively high helical content.[29–31] OX-B comprises two α-helices spanning residues Leu7-Gly19 (helix I) and Ala23-Met28 (helix II), respectively. A flexible linker (residues Asn20 and His21) connects them orienting their axis about 60-80° relative to one another (PDB ID:1CQ0) (**Figure 1.A**).[29] OX-A shows similar structural features to OX-B, however its N-terminus contains a third helix located between residues Cys6-Gln9 (helix III) and conformationally restrained by two disulfide bridges (PDB ID:1WSO) (**Figure 1.B**).[31]

So far, stapling with a photoswitchable crosslinker has enabled light-regulation over the secondary structure of helical peptides to control of a diversity of cellular processes.[32–37] However, the presence of two disulfide bonds in OX-A proved incompatible with peptide stapling,[38] whereas their reduction caused a nearly 10-fold loss in agonist activity towards both orexin receptors.[39–42] Orexin analogues mutated or truncated between Ala23 and Met28 are inactive, indicating that intracellular Ca^{2+} mobilization is due to the peptide C-terminus.[41,43,44]

Recently, Hong *et al*. determined the activated-state structure of OX_2 by cryo-electron microscopy (EM) and confirmed that OX-B C-terminus (helix II) is anchored deep into the receptor binding pocket.[45] In contrast, the flexible linker that connects the two helices is oriented towards the surface of the receptor and puts the hydrophobic face of helix I in contact with OX_2 extra cellular loop (ECL) 2 and N-terminus.[44–46] Surprisingly, the authors also found that OX-B C-terminal segment binds to the receptor in an extended conformation rather than adopting a helical structure. Considering both the technical hurdles and the limited impact of photoregulating orexin helicity,[47] we reasoned that replacing the flexible hinge of OX-B with a photoswitchable amino acid might allow to reversibly disrupt the overall geometry of the ligand.

Consequently, we designed a photoswitchable analogue of orexin-B as follows: i) Asn20 and His21 were replaced by an ω-amino acid containing an azobenzene moiety; ii) the linear sequence of the peptide was reduced to the minimum required for receptor activation (OX-B$_{6-28}$) by removing the N-terminus; and iii) the C-terminal amidation was maintained as beneficial for both peptide activity and stability (**Figure 1.B**). As molecular switch, we chose [3-(3-aminomethyl)phenylazo]phenylacetic acid (AMPP) (**Figure 1.C**). This choice took into account the excellent photochromic properties of azobenzene, the possibility to obtain great alterations in geometry upon photoisomerization, and several successful reports where the switch component had been inserted into β-turns and within α-helices to photoregulate the orientation of the associated secondary structures.[48–51] In addition, the two methylene bridges adjacent to the azobenzene core could guarantee enough flexibility to the system.[52]

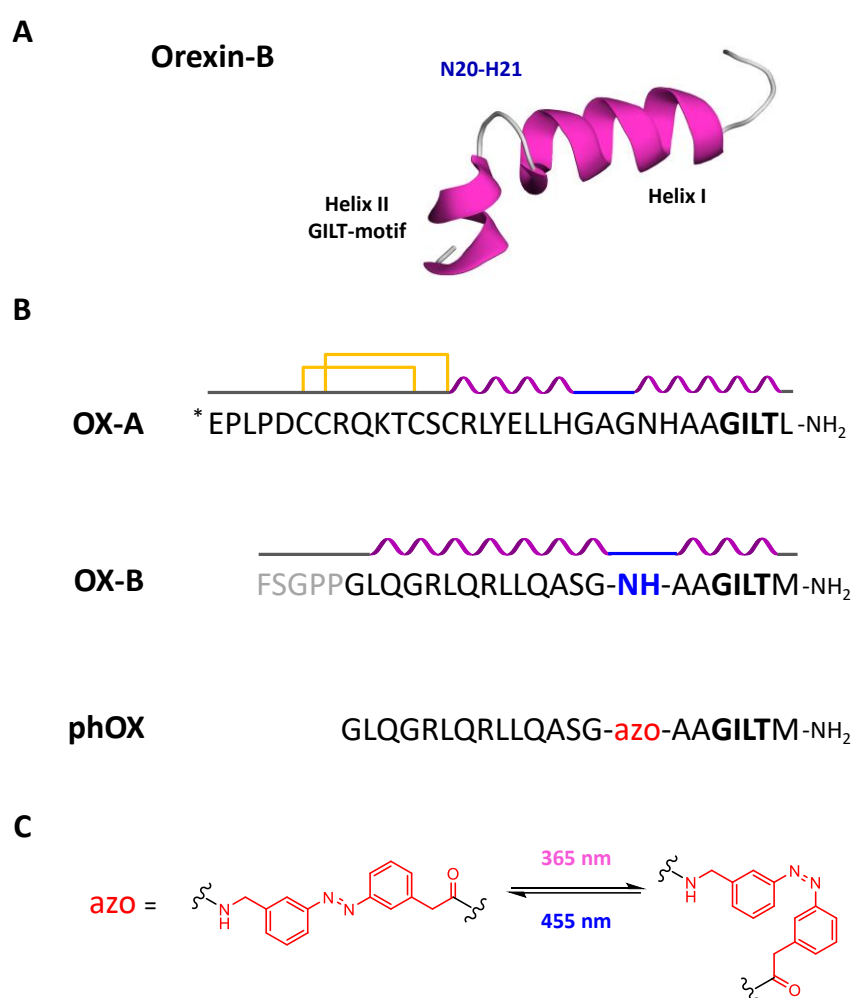**Figure 1 Rational design of photorexin (phOX) A)** NMR-derived solution structure of the orexin-B peptide (PDB: 1CQ0). A flexible linker (N20 and H21) is located between Helix I (L7-G19) and the biologically active GILT-motif in Helix II (A23-M28). **B)** Comparison of the amino acid sequences and secondary structures of orexin-A (OX-A), orexin-B (OX-B), and photorexin (phOX). In the latter, the unstructured N-terminus (in grey in OX-B) was removed, while the flexible linker (N20 and H21, in blue in OX-B) was replaced with a photoswitchable amino acid (azo, in red in phOX). *E represents pyroglutamic acid, C-termini are amidated. In the scheme, α-helices are pictured in purple, turns are shown in blue, and intramolecular disulfide bridges as yellow lines. **C)** *Trans* and *cis* structures of the photoswitchable ω-amino acid [3-(3-aminomethyl)phenyl-azo] phenylacetic acid (AMPP, in red).

Fmoc-protected AMPP was synthesized as reported in the literature and incorporated into the backbone of photorexin (phOX) combining automated and manual solid-phase peptide synthesis (SPPS) with a standard Fmoc-based strategy.[50] Insertion of the azo-amino acid was confirmed by UV-Vis spectroscopy (**Figure S2.1**). Furthermore, taking advantage of the thermal bistability reported for this azobenzene,[51] the photochromism of photorexin was fully characterized by UPLC analysis. Thus, the percentages of the two isomers were quantified while testing a variety of illumination conditions. In particular, we studied switching kinetics and photostationary states using 311, 365, and 380 nm UV light for the *trans→cis* photoisomerization (**Figure 2.A**); and 455 and 500 nm visible light (blue and green, respectively) for the reverse process (*cis→trans*) (**Figure 2.B**).

Trans photorexin could be readily converted to the *cis* isomer by illuminating between 311 and 365 nm, whereas the extent of photoisomerization was lower at longer wavelengths (e.g. 380 nm). From an initial photostationary state of 13% *cis* and 87% *trans* under benchtop conditions, an excellent 20:80 (*trans:cis*) ratio was achieved after 2 minutes of illumination at 365 nm (**Figure 2.A**). In contrast, exposure to blue light during 3 minutes back-isomerized the compound and reverted the ratio to 74:26 (*trans:cis*). Similar values could also be reached illuminating with green light for a longer time (~ 5 min) (**Figure 2.B**).

We then tested the photochromic stability of our peptide. Photorexin could be readily toggled between 87% *cis* and 74% *trans* with alternating cycles of UV and blue light of 3 minutes each. The process was repeated several times without significant degradation or bleaching (**Figure 2.C**). Finally, the thermal relaxation of the *cis* isomer ($t_{1/2}$ ~ 23 hours at 25°C) was determined as displayed in **Figure 2.D**.

It must be noted that although UV wavelengths required to photoswitch our peptide do not penetrate deep into tissue, symmetric azobenzenes like AMPP can also be isomerized with mid-infrared light using three-photon excitation. This method offers deep penetration and three-dimensional focusing on the microscale.[53]
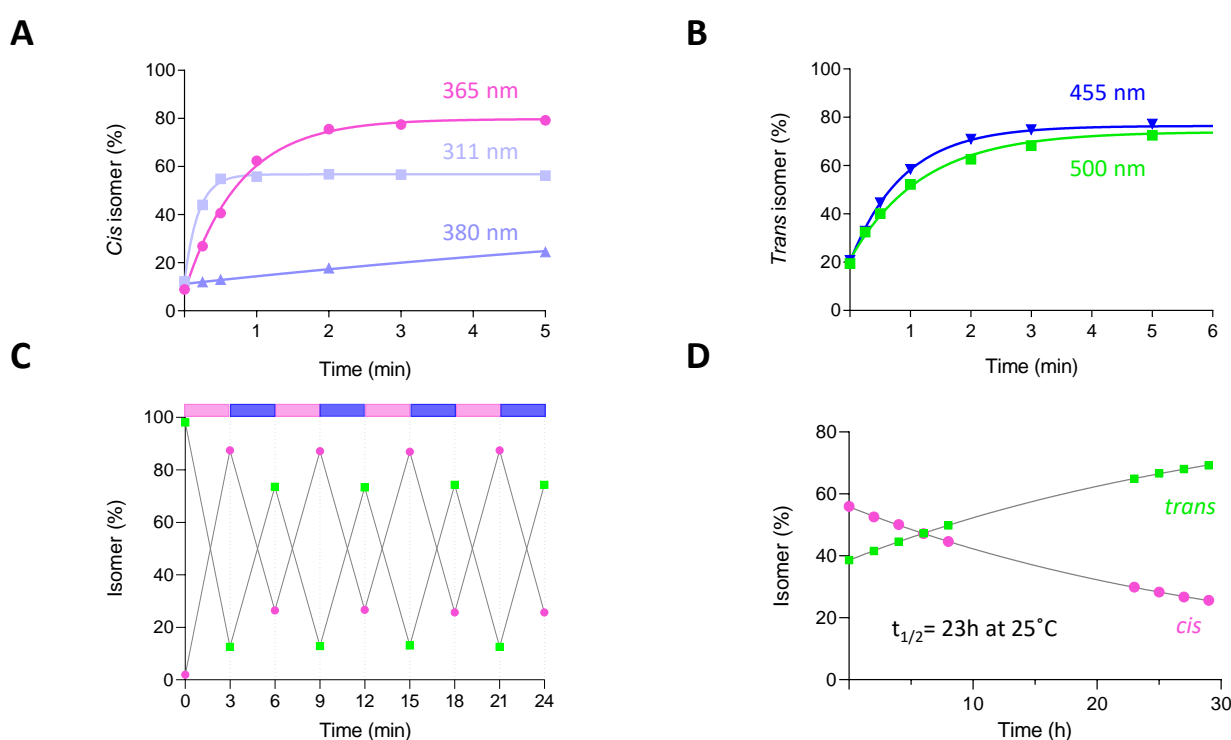

Figure 2 Photorexin photochromic characterization. A-B) Isomeric distribution of a phOX sample (50 μM in PBS at pH 7.4 and 25°C) when photoswitching from *trans* to *cis* (**A**) or from *cis* to *trans* (**B**) after cumulative illumination at different wavelengths. Percentages of the two species were quantitatively determined by UPLC analysis upon resolving the peak of the two isomers at given illumination times. Data were fitted to a monoexponential decay model. **C)** Reversibility and stability of the photochromic behavior of phOX (25 μM in PBS at pH 7.4 and 25°C) over several cycles (3 minutes each) of photoinduced isomerization at 365 nm (*trans→cis*) and 455 nm (*cis→trans*). Percentages of the two isomers were determined by UPLC analysis after each cycle. **D)** Thermal relaxation of phOX at 25°C in PBS (pH 7.4) as monitored by UPLC analysis. Data were fitted to a monoexponential decay model for *cis* half-life determination.

Photorexin pharmacodynamics were then examined to understand: i) how replacement of the flexible hinge with the photoswitchable AMPP amino acid affected both potency and maximal efficacy of the peptide; and ii) to which extent these properties could be photoregulated. Given the convenient bistability of the two isomers, pre-illuminated samples were tested using an *in vitro* functional assay that monitors real-time intracellular calcium responses through the FLIPR Tetra system.

Activity was evaluated either in CHO-K1 cells stably transfected with the human OX_1 receptor or in PFSK-1 cells. The latter is a human neuroectodermal cell line, derived from a brain tumor, that innately expresses the hOX_2 receptor. Both orexin-B and our photoswitchable analogue increased calcium release in a concentration-dependent manner, unambiguously indicating agonist activity (**Figure S3.2**). The potency of the native peptide was consistent with reported values.[10,42] Promisingly, photorexin retained high maximal efficacy and nanomolar activity towards both receptor subtypes. The EC_{50} of *trans* photorexin at hOX_2 was only 4-fold shifted to the right compared to the dose-response curve of the endogenous peptide. This reduction in potency was slightly higher at hOX_1, where *trans* photorexin displayed a 9-fold decrease in activity (**Table S3.1**).

Despite modest light-induced changes, *trans* photorexin consistently exhibited statistically significant higher potency compared to the *cis* isomer (1.4-fold and 2.0-fold at OX_1 and OX_2, respectively). As the calcium-sensitive dye used in the assay requires 470-495 nm excitation, blue light was likely to back-isomerize pre-illuminated *cis* photorexin to *trans*, thereby reducing any difference in activity between the two samples. To overcome this limitation, we decided to assess intracellular calcium responses in a different system.

Calcium fluorescence imaging also allows to quantify real-time changes in the cytosolic calcium concentration, but with single-cell or subcellular resolution. As it relies on exogenous indicators, we chose a genetically encoded calcium indicator that could be excited with green light (R-GECO1, λ_{ex} = 562 nm). In addition to overcoming the beforementioned limitations of blue light excitation, R-GECO1 red-shifted absorption spectrum offered the possibility of photoisomerizing the peptide *in situ*, which proved advantageous compared to testing only pre-irradiated samples.

Photorexin was first applied as a control to TsA201 cells transfected only with the calcium indicator. The absence of response to the compound and concomitant UV or blue illumination ruled out light-induced artifacts due to non-specific R-GECO1 stimulation (**Figure S3.3**). Subsequently, 100 nM photorexin was applied to cells co-transfected with R-GECO1 and GFP-labelled hOX_2. The peptide evoked a sharp transient response in the dark, displaying oscillations with a period of 1-3 min depending on each cell. Illumination with UV light terminated these responses in a few seconds, and oscillatory activity was resumed upon exposure to blue light (**Figure 3.A-B**). Similar patterns of calcium signals could be reproduced in at least two cycles of alternating UV and visible light as well as at lower doses (30 nM, **Figure S3.4**), thus demonstrating that photorexin can robustly and reversibly regulate the activity of orexin receptors with light and that it behaves as a *trans*-active agonist with nanomolar potency. The dynamic photocontrol of orexin receptor activity enabled by photorexin is in contrast to the irreversible photo-release of caged OX-B demonstrated *in vitro*.[54] In hOX_1-expressing cells, the dark-adapted peptide also produced an increase in calcium influx, although smaller in magnitude than in TsA201-hOX_2. UV- and blue-light illumination (365 and 455 nm, respectively) elicited no effect (**Figure 3.C** and **Figure S3.5**).

Calcium traces from different cells were then integrated to quantify the observed responses. Noticeably, *cis* photorexin retained only 6% of the dark-adapted peptide activity towards hOX_2. While illumination with blue light rapidly restored calcium mobilization, recovery was partial (52% of the initial responses) probably owing to receptor desensitization after prolonged agonist exposure (**Figure 3.D**). In the dose-response curves, dark-adapted photorexin displayed significantly lower potency towards hOX_1, whereas both the UV- and blue-light illuminated forms evoked no response on this receptor, thus demonstrating selectivity towards hOX_2 (**Figure S3.5** and **Figure 3.E**). In light of the promising results obtained through calcium fluorescence, we moved on to test photorexin activity *in vivo*.
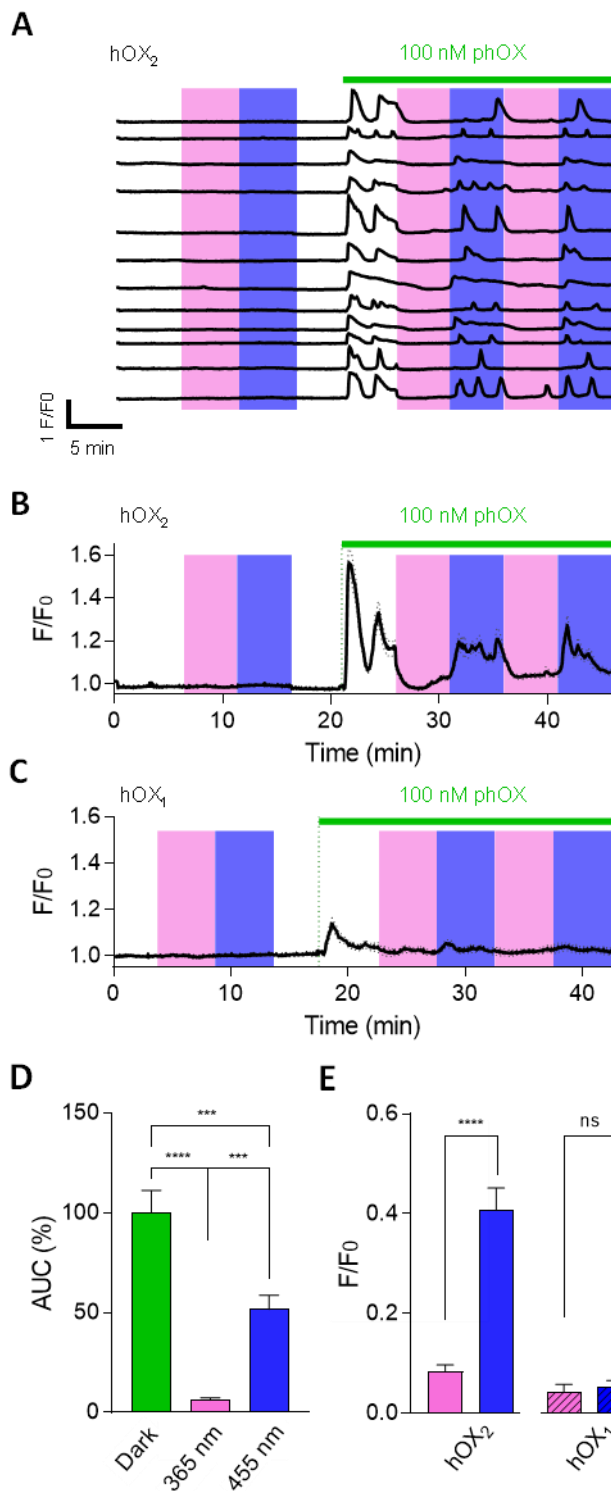
Figure 3 Photorexin pharmacodynamics A) Representative single-cell calcium traces (*n*=12) in TsA201 cells transiently expressing GFP-hOX$_2$ and R-GECO1. Upon application of 100 nM photorexin (green bar) in its dark-adapted state (*trans,* white area) cells gave sharp responses. Calcium oscillations were then abolished upon exposure to cycles of UV light (365 nm, *cis*-enriched state in pink) and recovered with blue illumination (455 nm, *trans*-enriched state in blue). **B)** Real-time intracellular calcium recordings (averaged traces, black line, *n*=20) from TsA201 cells co-expressing hOX$_2$ and R-GECO1 upon application of 100 nM photorexin (green bar). Traces were recorded in the dark (white area) and under cycles of illumination with UV (365 nm, pink) and blue (455 nm, blue) light. Grey dotted band represents ± SEM. **C)** Real-time calcium imaging responses (averaged traces, black line, *n*=20 cells) from TsA201 cells co-expressing hOX$_1$ and R-GECO1. Application of photorexin (100 nM, green bar) evokes mild responses in the dark and under blue light. Gray bars represent ± SEM. **D)** Efficacy of phOX (100 nM) on TsA201-hOX$_2$ quantified in the dark (green bar) and after subsequent illumination with 365 nm UV light (pink bar, *cis* enriched) and back-isomerization to *trans* with 455 nm blue light (blue bar). Responses were quantified as Area Under the Curve (AUC) and normalized to those obtained with dark-adapted phOX. Data represent means ± SEM (*n*=20 cells). Statistical differences were determined by one-way ANOVA with Tukey's multiple comparison test. (***, *p*-value ≤ 0.001; ****, *p*-value ≤ 0.0001). **E)** Selectivity of phOX (100 nM) over TsA201-hOX$_2$ (full-coloured bars) and TsA201-hOX$_1$ (dashed bars) compared after illumination with 365 nm UV light (*cis* enriched, in pink) and after back-isomerization to *trans* with 455 nm blue light (in blue). Data represent amplitude means ± SEM (*n*=20 cells). Statistical differences were determined by one-way ANOVA with paired-sample Wilcoxon signed rank test (ns, not significant; ****, *p*-value ≤ 0.0001).

The orexin neural network in zebrafish has been studied in detail and, as in mammals, it is involved in many physiological functions including sleep/wake cycles, homeostasis, feeding, and locomotor activity.[55–60] Between 16 and 60 neurons compose the zebrafish's network with a similar gene to mammals encoding for two orexins neuropeptides (OX-A/-B).[59] Only one orexin receptor has been found in zebrafish, closely related to mammalian OX$_2$ (70%). Its binding pocket is highly conserved throughout species.[13,59] The simplicity of the network in zebrafish and its close resemblance to higher mammals, along with the advantages of using an established neuropharmacological[61–64] and photopharmacological[5,65] animal model, allowed us to investigate the effects of photorexin on locomotor activities of wildtype larvae.

Individual larvae were placed in separate wells of a 96 well plate, each containing increasing concentrations of photorexin. Each individual was tracked and monitored over 68 minutes under different illumination conditions, alternating between 365 nm, 455 nm, and dark periods (respectively indicated by purple, blue, and grey in **Figure 4.A**). The time course of 12 larvae per concentration group integrated every minute are shown in **Figure 4.A**. All applied concentrations are shown in **Figure 4.B** (0-10 µM).

High doses of photorexin (1 and 10 µM) significantly enhanced locomotion (distance swum over 1-min integration intervals) under 365 nm light in comparison to non-treated larva, for all UV illuminated periods. This increase in activity was sharply reverted under visible blue light and all treated larvae swum distances similar to non-treated individuals. Interestingly, the successive induction reflex (i.e., the fast increase and slow decrease in locomotion observed upon switching off visible light)[66,67] is significantly reduced for all photorexin-treated groups in comparison to controls as observed at t = 49 min (**Figure 4.A**). These findings are consistent with sleep behaviors in zebrafish after exposure to orexin agonists, that elicit lower responsiveness upon light-to-dark changes.[58]

It must be noted that rodents have been the model of choice to develop hypnotics and psychostimulants despite their different sleep patterns to humans. As an alternative, zebrafish larvae show peak daytime activity and rest at night, are cost-effective, and amenable to high throughput screening as shown in **Figure 4**.
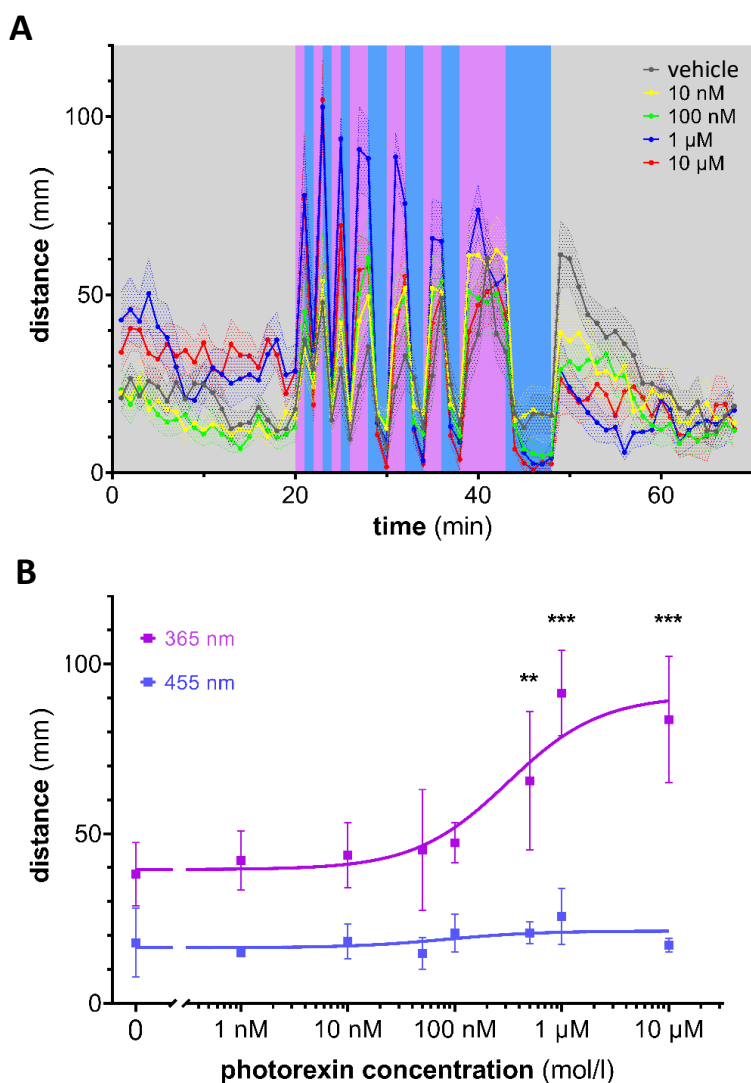

Figure 4 Photorexin *in vivo* activity in wildtype zebrafish A) Fast-swimming distances (faster than 6 mm·s⁻¹) are plotted for larvae treated with different doses of phOX (vehicle – dark gray, 10 nM - yellow, 100 nM – green, 1 µM – blue, and 10 µM – red traces). Distances were integrated over 1-min intervals. UV illumination periods increased swimming activity of larvae exposed to high phOX doses (1 and 10 µM), while blue light reversed activity to levels of non-treated larvae. This different behavior was maintained over several light cycles. After the last illumination interval (5 min at 455 nm), all treated larvae showed a weaker induction response (i.e., the fast increase and slow decrease in locomotion observed upon switching off visible light). Patterned areas represent ± SEM (*n*=12 larvae per condition). **B)** Dose-response curves (distance swum in mm) in zebrafish larvae of *cis* (365 nm, in purple) and *trans* (455 nm, in blue) phOX upon integrating the 3 consecutive 1-min illumination intervals between minutes 20 and 26 for each wavelength (365 nm and 455 nm, purple and blue traces respectively). Error bars represent ± SD (*n* = 12 larvae per treatment group). Solid traces are fits to log(agonist) vs. response model. Statistical differences were determined by two-way ANOVA with Tukey's multiple comparison test (**, *p*-value ≤ 0.01; ***, *p*-value ≤ 0.001).

Overall, both *in vitro* and *in vivo* results validate the rationale behind our photoswitchable peptide ligand design. While interventions at the flexible hinge are compatible with preserving the functional activity of the peptide, peptide ligands require proper orientation of the axis to ensure receptor agonism and intracellular signaling. This achievement offers the ability to control endogenous orexin receptors remotely and in the different regions of the brain that receive orexinergic projections, and allows reversible and repeatable activation of orexin receptors at high temporal resolution to investigate gating mechanisms. To examine this question, we further studied photorexin structures associated to the observed differences in receptor activity.

In order to correlate the functional potencies of the *trans* and *cis* isomers with their respective conformations, we performed circular dichroism (CD) studies and molecular dynamics calculations. Photorexin CD spectra in phosphate buffer saline displayed a strong positive band at 195 nm and a negative one at 218 nm (**Figure S4.1A**). This behavior suggests the presence of a nascent α-helix. In the presence of 30% trifluoroethanol (TFE), the spectra revealed enhanced helicity (40%) with a negative band at 207 nm and a shoulder at 220 nm (**Figure S4.1B**).[41] Moreover, while photorexin in 30% TFE was not affected by light-induced photoisomerization of AMPP, the CD spectrum recorded in PBS displayed a loss in secondary structure after exposure to UV light. Despite the variation being mild, we investigated if the detected structural changes were restricted to photorexin helix I or helix II and could partially account for the loss of potency of the *cis* isomer.

We thus performed replica exchange with solute tempering (REST) molecular dynamics simulations in explicit water to analyze the secondary structures of *trans* and *cis* photorexin and to relate them to their closest non-photoswitchable analogue (truncated OX-B, residues 6-28, with no amino acid replacement at the flexible hinge). Atom coordinates were extracted from the solution structure reported by Lee *et al.* (PDB ID: 1CQ0)[29] and we manually modified them to truncate the N-terminus and, in the case of our analogues, insert those of NMR-solved *trans* and *cis* AMPP (PDB ID: 2H4B).[68] As an indicator of helicity, the average number of backbone H-bonds formed during the simulations was plotted for helix I (Gly6-Gly19) and helix II (Ala23-Met28) and compared between the three analogues (**Figure S4.2**). Additionally, dihedral angles of residues at helix I and helix II were analyzed for the 300 K trajectory as a complementary indication of secondary structure (**Figure S4.3A-B**). Surprisingly, no significant variations in helicity content and/or in the conformational preferences of the residues were observed among the three analogues. Thus, the difference in activity observed between *trans* and *cis* photorexin cannot be directly attributed to partial losses in secondary structure.

As photoisomerization was expected to affect the spatial arrangement of the two helices, we moved on to study the evolution of the intramolecular helix I - helix II angle. During REST simulations, all the peptides displayed a high degree of "hinge" flexibility which resulted in significant angle fluctuations. However, while OX-B$_{(6-28)}$ helices were on average inclined at 45° (**Figure S4.4A**), the angles in *cis* and *trans* phOX were both closer to 90° (**Figure S4.4B-C**), thus suggesting that: i) the azobenzene moiety prevents closing of the inter-helix angle compared to the flexible hinge of the native peptide; and ii) its photoisomerization does not further influence the angle between the two peptide fragments.

Finally, we analyzed the main clusters of conformations explored by each molecule during the 200 ns REST simulations. The most populated conformations for each derivative were locally aligned by the backbone of helix II - GILT- residues, as these constitute the hotspots for receptor binding and activation.[69] As observed from the alignment, *trans* photorexin (in green) preferentially places helix I in a similar orientation as for OX-B$_{(6-28)}$ (in grey) (**Figure S4.5**). In contrast, helix I of the *cis* isomer (in pink) is orientated in the opposite direction.

As previously demonstrated by mutagenesis studies and recently supported by cryo-EM, the α-helical N-termini of OX-B and OX$_2$ as well as the ECL-2 of the latter actively engage in the formation of the receptor-peptide complex through a "message-address system" based on polytopic interactions.[45,70] According to this model, the N-terminus of the peptide directs binding to the receptor, whereas the "message" C-terminus conveys the functional information.[71–74] In addition, multiple weak interactions mediate affinity towards the receptors, overall contributing to the nM potency of the peptide.[70]

Among these hotspots for receptor binding and activation, two key residues (Leu16 and Leu20) have been identified to form a hydrophobic patch located on helix I.[75,76] Our functional and structural data converge on

attributing the lower activity displayed by *cis* photorexin to the reverse orientation adopted by its N-terminus relative to the receptor binding pocket. In particular, the UV-illuminated analogue might be unable to establish productive hydrophobic interactions, such as those predicted between the beforementioned leucine residues and Phe346 and His350 located on the extracellular region of OX_2 (**Figure S4.6**).[75,77]

Conclusions

In conclusion, we have rationally designed and developed a reliable and efficient molecular tool to photocontrol orexinergic neurotransmission. Photorexin shows that introducing a photoswitchable amino acid into the backbone of signaling peptides allows for regulating their activity *in vitro* and *in vivo* by controlling the spatial arrangement of their C- and N- terminal fragments.[51] Potentially, this approach could be extended to a broad family of neuropeptides that share a "message-address" mechanism when binding to their cognate receptors.[71–74] Our light-regulated analogue retains elevated maximal efficacy, nanomolar activity, and selectivity towards hOX_2, thus showing that interventions at the flexible hinge are compatible with preserving the functional activity of the peptide. The long thermal stability and low intrinsic activity of the *cis* isomer enable administration and subsequent activation of the compound with blue light, thus offering unprecedented spatiotemporal precision to manipulate orexinergic circuits. Photorexin is the first photo-reversible ligand reported for orexin receptors. It allows dynamic control of activity *in vitro* and in zebrafish larvae by direct application in water. Photorexin induces dose- and light-dependent changes in locomotion and a reduction in the successive induction reflex that is associated to sleep behavior.

1. Lee, C., Lavoie, A., Liu, J., Chen, S. X. & Liu, B. Light Up the Brain: The Application of Optogenetics in Cell-Type Specific Dissection of Mouse Brain Circuits. *Front. Neural Circuits* **14**, (2020).

2. Kim, C. K., Adhikari, A. & Deisseroth, K. Integration of optogenetics with complementary methodologies in systems neuroscience. *Nat. Rev. Neurosci.* **18**, 222–235 (2017).

3. Deisseroth, K. Optogenetics: 10 years of microbial opsins in neuroscience. *Nat. Neurosci.* **18**, 1213–1225 (2015).

4. Zalocusky, K. A., Fenno, L. E. & Deisseroth, K. Current challenges in optogenetics. *Optogenetics* 23–33 (2013) doi:10.1515/9783110270723.23.

5. Hüll, K., Morstein, J. & Trauner, D. In vivo photopharmacology. *Chem. Rev.* **118**, 10710–10747 (2018).

6. Lerch, M. M., Hansen, M. J., van Dam, G. M., Szymanski, W. & Feringa, B. L. Emerging targets in photopharmacology. *Angew. Chemie - Int. Ed.* **55**, 10978–10999 (2016).

7. Velema, W. A., Szymanski, W. & Feringa, B. L. Photopharmacology: Beyond proof of principle. *J. Am. Chem. Soc.* **136**, 2178–2191 (2014).

8. Fuchter, M. J. On the Promise of Photopharmacology Using Photoswitches: A Medicinal Chemist's Perspective. *J. Med. Chem.* **63**, 11436–11447 (2020).

9. Morstein, J., Awale, M., Reymond, J. L. & Trauner, D. Mapping the Azolog Space Enables the Optical Control of New Biological Targets. *ACS Cent. Sci.* **5**, 607–618 (2019).

10. Sakurai, T. *et al.* Orexins and orexin receptors: A family of hypothalamic neuropeptides and G protein-coupled receptors that regulate feeding behavior. *Cell* **92**, 573–585 (1998).

11. De Lecea, L. *et al.* The hypocretins: Hypothalamus-specific peptides with neuroexcitatory activity. *Proc. Natl. Acad. Sci. U. S. A.* **95**, 322–327 (1998).

12. Sakurai, T. The neural circuit of orexin (hypocretin): Maintaining sleep and wakefulness. *Nature Reviews Neuroscience* vol. 8 171–181 (2007).

13. Wong, K. K. Y., Ng, S. Y. L., Lee, L. T. O., Ng, H. K. H. & Chow, B. K. C. Orexins and their receptors from fish to mammals: A comparative approach. *Gen. Comp. Endocrinol.* **171**, 124–130 (2011).

14. Nambu, T. *et al.* Distribution of orexin neurons in the adult rat brain. (1999).

15. Peyron, C. *et al.* Neurons Containing Hypocretin (Orexin) Project to Multiple Neuronal Systems. *J. Neurosci.* **18**, 9996–10015 (1998).

16. Van Den Pol, A. N., Gao, X. B., Obrietan, K., Kilduff, T. S. & Belousov, A. B. Presynaptic and postsynaptic actions and modulation of neuroendocrine neurons by a new hypothalamic peptide, hypocretin/orexin. *J. Neurosci.* **18**, 7962–7971 (1998).

17. Kukkonen, J. P. & Leonard, C. S. Orexin/hypocretin receptor signalling cascades. *Br. J. Pharmacol.* **171**, 314–331 (2014).

18. Brisbare-Roch, C. *et al.* Promotion of sleep by targeting the orexin system in rats, dogs and humans. *Nat. Med.* **13**, 150–155 (2007).

19. Scammel, T. R. & Winrow, C. Orexin Receptors: Pharmacology and Therapeutic Opportunities. *Annu Rev Pharmacol Toxicol.* **10**, 243–266 (2011).

20. Lin, L. *et al.* The Sleep Disorder Canine Narcolepsy Is Caused by a Mutation in the Hypocretin (Orexin) Receptor 2 Gene. *Cell* **98**, 365–376 (1999).

21. Thannickal, T. C. *et al.* Reduced number of hypocretin neurons in human narcolepsy. *Neuron* **27**, 469–474 (2000).

22. Peyron, C. *et al.* A mutation in a case of early onset narcolepsy and a generalized absence of hypocretin peptides in human narcoleptic brains. *Nat. Med.* **6**, 991–997 (2000).

23. Nagahara, T. *et al.* Design and Synthesis of Non-Peptide, Selective Orexin Receptor 2 Agonists. *J. Med. Chem.* **58**, 7931–7937 (2015).

24. Irukayama-Tomobe, Y. *et al.* Nonpeptide orexin type-2 receptor agonist ameliorates narcolepsy-cataplexy symptoms in mouse models. *Proc. Natl. Acad. Sci. U. S. A.* **114**, 5731–5736 (2017).

25. Yukitake, H. *et al.* TAK-925, an orexin 2 receptor-selective agonist, shows robust wake-promoting effects in mice. *Pharmacol. Biochem. Behav.* **187**, 172794 (2019).

26. Turku, A. *et al.* Pharmacophore Model to Discover OX 1 and OX 2 Orexin Receptor Ligands. *J. Med. Chem.* **59**, 8263–8275 (2016).

27. Pittolo, S. *et al.* An allosteric modulator to control endogenous G protein-coupled receptors with light. *Nat. Chem. Biol.* **10**, 813–815 (2014).

28. Schoenberger, M., Damijonaitis, A., Zhang, Z., Nagel, D. & Trauner, D. Development of a new photochromic ion channel blocker via azologization of fomocaine. *ACS Chem. Neurosci.* **5**, 514–518 (2014).

29. Lee, J. H. *et al.* Solution structure of a new hypothalamic neuropeptide, human hypocretin- 2/orexin-B. *Eur. J. Biochem.* **266**, 831–839 (1999).

30. Kim, H. Y., Hong, E., Kim, J. Il & Lee, W. Solution structure of human orexin-A: Regulator of appetite and wakefulness. *J. Biochem. Mol. Biol.* **37**, 565–573 (2004).

31. Takai, T. *et al.* Orexin-A is composed of a highly conserved C-terminal and a specific, hydrophilic N-terminal region, revealing the structural basis of specific recognition by the orexin-1 receptor. *J. Pept. Sci.* **12**, 443–454 (2006).

32. Guerrero, L. *et al.* Photochemical regulation of DNA-binding specificity of MyoD. *Angew. Chemie - Int. Ed.* **44**, 7778–7782 (2005).

33. Kneissl, S., Loveridge, E. J., Williams, C., Crump, M. P. & Allemann, R. K. Photocontrollable peptide-based switches target the anti-apoptotic protein Bcl-xL. *Chembiochem* **9**, 3046–3054 (2008).

34. Zhang, F., Timm, K. A., Arndt, K. M. & Woolley, G. A. Photocontrol of coiled-coil proteins in living cells. *Angew. Chemie - Int. Ed.* **49**, 3943–3946 (2010).

35. Nevola, L. *et al.* Light-regulated stapled peptides to inhibit protein-protein interactions involved in clathrin-mediated endocytosis. *Angew. Chemie - Int. Ed.* **52**, 7704–7708 (2013).

36. Martín-Quirós, A. *et al.* Absence of a stable secondary structure is not a limitation for photoswitchable inhibitors of β-arrestin/β-adaptin 2 protein-protein interaction. *Chem. Biol.* **22**, 31–37 (2015).

37. Prischich, D. *et al.* Light-dependent inhibition of clathrin-mediated endocytosis in yeast unveils conserved functions of the AP2 complex. *iScience* **26**, 107899 (2023).

38. Burns, D. C., Zhang, F. & Woolley, G. A. Synthesis of 3,3'-bis(sulfonato)-4,4'-bis(chloroacetamido) azobenzene and cysteine cross-linking for photo-control of protein conformation and activity. *Nat. Protoc.* **2**, 251–258 (2007).

39. Okumura, T. *et al.* Requirement of intact disulfide bonds in orexin-A-induced stimulation of gastric acid secretion that is mediated by OX1 receptor activation. *Biochem. Biophys. Res. Commun.* **280**, 976–981 (2001).

40. Darker, J. G. *et al.* Structure-activity analysis of truncated orexin-A analogues at the orexin-1 receptor. *Bioorganic Med. Chem. Lett.* **11**, 737–740 (2001).

41. Lang, M. *et al.* Structural properties of orexins for activation of their receptors. *J. Pept. Sci.* **12**, 258–266 (2006).

42. Lang, M., Söll, R. M., Dürrenberger, F., Dautzenberg, F. M. & Beck-Sickinger, A. G. Structure-Activity Studies of Orexin A and Orexin B at the Human Orexin 1 and Orexin 2 Receptors Led to Orexin 2 Receptor Selective and Orexin 1 Receptor Preferring Ligands. *J. Med. Chem.* **47**, 1153–1160 (2004).

43. Asahi, S. *et al.* Development of an orexin-2 receptor selective agonist, [Ala11, D-Leu15]orexin-B. *Bioorganic Med. Chem. Lett.* **13**, 111–113 (2003).

44. Nicole, P., Couvineau, P., Jamin, N., Voisin, T. & Couvineau, A. Crucial role of the orexin-B C-terminus in the induction of OX1 receptor-mediated apoptosis: Analysis by alanine scanning, molecular modelling and site-directed mutagenesis. *Br. J. Pharmacol.* **172**, 5211–5223 (2015).

45. Hong, C. *et al.* Structures of active-state orexin receptor 2 rationalize peptide and small-molecule agonist recognition and receptor activation. *Nat. Commun.* **12**, (2021).

46. Heifetz, A. *et al.* Study of human orexin-1 and -2 G-protein-coupled receptors with novel and published antagonists by modeling, molecular dynamics simulations, and site-directed mutagenesis. *Biochemistry* **51**, 3178–3197 (2012).

47. Karhu, L. *et al.* Stapled truncated orexin peptides as orexin receptor agonists. *Peptides* **102**, 54–60 (2018).

48. Hoppmann, C. *et al.* Light-directed protein binding of a biologically relevant β-sheet. *Angew. Chemie - Int. Ed.* **48**, 6636–6639 (2009).

49. Hoppmann, C. *et al.* Photocontrol of contracting muscle fibers. *Angew. Chemie - Int. Ed.* **50**, 7699–7702 (2011).

50. Podewin, T. *et al.* Photocontrolled chignolin-derived β-hairpin peptidomimetics. *Chem. Commun.* **51**, 4001–4004 (2015).

51. Broichhagen, J. *et al.* Optical Control of Insulin Secretion Using an Incretin Switch. *Angew. Chemie - Int. Ed.* **54**, 15565–15569 (2015).

52. Dong, S. L. *et al.* A photocontrolled β-hairpin peptide. *Chem. - A Eur. J.* **12**, 1114–1120 (2006).

53. Sortino, R. *et al.* Three-Photon Infrared Stimulation of Endogenous Neuroreceptors in Vivo. *Angew. Chemie Int. Ed.* (2023) doi:10.1002/anie.202311181.

54. Duffet, L. *et al.* A photocaged orexin-B for spatiotemporally precise control of orexin signaling. *Cell Chem. Biol.* **29**, 1729-1738.e8 (2022).

55. Yokobori, E. *et al.* Stimulatory effect of intracerebroventricular administration of orexin A on food intake in the zebrafish, Danio rerio. *Peptides* **32**, 1357–1362 (2011).

56. Elbaz, I., Foulkes, N. S., Gothilf, Y. & Appelbaum, L. Circadian clocks, rhythmic synaptic plasticity and the sleep-wake cycle in zebrafish. *Front. Neural Circuits* **7**, 1–7 (2013).

57. Prober, D. A., Rihel, J., Onah, A. A., Sung, R. J. & Schier, A. F. Hypocretin/orexin overexpression

induces an insomnia-like phenotype in zebrafish. *J. Neurosci.* **26**, 13400–13410 (2006).

58. Pardon, M. *et al.* Modulation of sleep behavior in zebrafish larvae by pharmacological targeting of the orexin receptor. *Front. Pharmacol.* **13**, 1–14 (2022).

59. Lawrence, A. J. & De Lecea, L. *Behavioral Neuroscience of Orexin/Hypocretin, vol. 33*. (2017).

60. Yokogawa, T. *et al.* Characterization of Sleep in Zebrafish and Insomnia in Hypocretin Receptor Mutants. *PLoS Biol.* **5**, 2379–2397 (2007).

61. Kalueff, A. V., Stewart, A. M. & Gerlai, R. Zebrafish as an emerging model for studying complex brain disorders. *Trends Pharmacol. Sci.* **35**, 63–75 (2014).

62. Khan, K. M. *et al.* Zebrafish models in neuropsychopharmacology and CNS drug discovery. *Br. J. Pharmacol.* **174**, 1925–1944 (2017).

63. Basnet, R. M., Zizioli, D., Taweedet, S., Finazzi, D. & Memo, M. Zebrafish larvae as a behavioral model in neuropharmacology. *Biomedicines* **7**, (2019).

64. Cassar, S. *et al.* Use of Zebrafish in Drug Discovery Toxicology. *Chem. Res. Toxicol.* **33**, 95–118 (2020).

65. Gomila, A. M. J. & Gorostiza, P. In Vivo Applications of Photoswitchable Bioactive Compounds. in *Molecular Photoswitches* 811–842 (Wiley, 2022). doi:10.1002/9783527827626.ch34.

66. Staddon, J., Macphail, R. & Padilla, S. Successive Induction in Larval Zebrafish. *Nat. Preced.* 1–13 (2009) doi:10.1038/npre.2009.3659.1.

67. Staddon, J. E. R., MacPhail, R. C. & Padilla, S. The dynamics of successive induction in larval zebrafish. *J. Exp. Anal. Behav.* **94**, 261–266 (2010).

68. Jurt, S., Aemissegger, A., Güntert, P., Zerbe, O. & Hilvert, D. A photoswitchable miniprotein based on the sequence of avian pancreatic polypeptide. *Angew. Chemie - Int. Ed.* **45**, 6297–6300 (2006).

69. Hong, C. *et al.* Structures of active-state orexin receptor 2 rationalize peptide and small-molecule agonist recognition and receptor activation. *Nat. Commun.* **12**, (2021).

70. Yin, J. *et al.* Structure and ligand-binding mechanism of the human OX 1 and OX 2 orexin receptors. *Nat. Struct. Mol. Biol.* **23**, 293–299 (2016).

71. Sakamoto, A. *et al.* The ligand-receptor interactions of the endothelin systems are mediated by distinct "message" and "address" domains. *J. Cardiovasc. Pharmacol.* **22**, S113–S116 (1993).

72. Guerrini, R. *et al.* Address and message sequences for the nociceptin receptor: A structure–activity study of nociceptin-(1–13)-peptide amide. *J. Med. Chem.* **40**, 1789–1793 (1997).

73. Paterlini, Portoghese, P. S. & Ferguson, D. M. Molecular simulation of dynorphin A-(1–10) binding to extracellular loop 2 of the κ-opioid receptor. A model for receptor activation. *J. Med. Chem.* **40**, 3254–3262 (1997).

74. della Longa, S. & Arcovito, A. A dynamic picture of the early events in nociceptin binding to the NOP receptor by metadynamics. *Biophys. J.* **111**, 1203–1213 (2016).

75. Heifetz, A. *et al.* Toward an understanding of agonist binding to human orexin-1 and orexin-2 receptors with G-protein-coupled receptor modeling and site-directed mutagenesis. *Biochemistry* **52**, 8246–8260 (2013).

76. Malherbe, P. *et al.* Mapping the binding pocket of dual antagonist almorexant to human orexin 1 and orexin 2 receptors: Comparison with the selective OX1 antagonist SB-674042 and the selective OX2

antagonist N-ethyl-2-[(6-methoxy- pyridin-3-yl)-(toluene-2-sulfonyl)-amino]-N-p. *Mol. Pharmacol.* **78**, 81–93 (2010).

77. Yin, J., Mobarec, J. C., Kolb, P. & Rosenbaum, D. M. Crystal structure of the human OX2 orexin receptor bound to the insomnia drug suvorexant. *Nature* **519**, 247–250 (2015).